

# 基质金属蛋白酶-2/9敏感型可跨膜融合抗氧化酶的表达、纯化和表征

何火聪<sup>2,3</sup>, 林丽香<sup>1,4</sup>, 李玲玲<sup>1,5</sup>, 吴伦巧<sup>1,6</sup>, 林海英<sup>1</sup>, 潘剑茹<sup>1</sup>

1 福州大学 生物科学与工程学院, 福建 福州 350108

2 福建医科大学附属肿瘤医院/福建省肿瘤医院 放射生物学及肿瘤放射治疗学研究室, 福建 福州 350014

3 福州大学 化学学院, 福建 福州 350108

4 雅博捷锐 (厦门) 医疗科技有限公司, 福建 厦门 361028

5 福州捷赫生物科技有限公司, 福建 福州 350108

6 深圳合民生物科技有限公司, 广东 深圳 518116

何火聪, 林丽香, 李玲玲, 吴伦巧, 林海英, 潘剑茹. 基质金属蛋白酶-2/9敏感型可跨膜融合抗氧化酶的表达、纯化和表征. 生物工程学报, 2022, 38(9): 3515-3527.

HE HC, LIN LX, LI LL, WU LQ, LIN HY, PAN JR. Expression, purification, and characterization of cell-permeable fusion antioxidant enzyme sensitive to matrix metalloproteinases-2/9. Chin J Biotech, 2022, 38(9): 3515-3527.

**摘要:** 融合了跨膜肽的抗氧化酶可进入细胞, 保护细胞免受放射损伤。然而跨膜肽的跨膜能力没有靶向性, 其也可把抗氧化酶带入肿瘤细胞进而保护肿瘤细胞, 降低放疗的效果。为此, 根据多数肿瘤细胞微环境中存在活性基质金属蛋白酶 (matrix metalloproteinase, MMP)-2 或 MMP-9 的特点, 在细胞跨膜肽 R9 与人铜、锌超氧化物歧化酶 (superoxide dismutase 1, SOD1) 和谷胱甘肽 S-转移酶 (glutathione S-transferase, GST) 之间融合 MMP-2/9 的底物肽 X, 设计了融合蛋白 GST-SOD1-X-R9。该蛋白在肿瘤微环境中可因 MMP-2/9 酶切底物肽 X 而失去跨膜肽, 从而无法进入肿瘤细胞, 进而只能进入正常细胞。全基因合成 SOD1-X-R9 序列, 并将其插入原核表达载体 pGEX-4T-1 中, 得到表达质粒, 并实现了 GST-SOD1-X-R9 融合蛋白的可溶表达。GST-SOD1-X-R9 经硫酸铵沉淀和 GST 亲和层析纯化, 分子量约为 47 kDa, 与理论值一致。纯化的融合蛋白的 SOD 活性和 GST 活性分别为 2 954 U/mg 和 328 U/mg。GST-SOD1-X-R9 的 SOD 活性或 GST 活性在生理条件下几乎没有变化。该融合蛋白在溶液中可被胶原酶 IV 部分水解。分别建立了 2D 和 3D 培养

**Received:** January 19, 2022; **Accepted:** May 10, 2022

**Supported by:** National Natural Science Foundation of China (81974482); Natural Science Foundation of Fujian Province, China (2019J01191, 2018J01732); the Fujian Provincial Health Technology Project (2019-CXB-8)

**Corresponding author:** PAN Jianru. Tel: +86-591-22866278; E-mail: panjr@fzu.edu.cn

**基金项目:** 国家自然科学基金 (81974482); 福建省自然科学基金 (2019J01191, 2018J01732); 福建省卫生健康科研人才培养项目 (2019-CXB-8)

的 HepG2 细胞模型来检验肿瘤微环境中的 MMP-2 活力对该蛋白跨膜能力的影响。在 2D 培养模型中, HepG2 的 MMP-2 活力极低, 但在 3D 培养模型中, 随着培养时间的增加, HepG2 肿瘤球的体积变大, 其胞外 MMP-2 活力也随之增强。GST-SOD1-X-R9 在 2D 培养的 HepG2 细胞中具有和 GST-SOD1-R9 蛋白一样的跨膜效率, 但在 3D 培养的 HepG2 细胞球中的跨膜能力大大降低。本研究为后续深入研究 GST-SOD1-X-R9 靶向防护正常细胞的氧化损伤效应奠定了基础。

**关键词:** 抗氧化酶; MMP-2/9 敏感性; 可跨膜; 大肠杆菌表达体系; 纯化; 稳定性

## Expression, purification, and characterization of cell-permeable fusion antioxidant enzyme sensitive to matrix metalloproteinases-2/9

HE Huocong<sup>2,3</sup>, LIN Lixiang<sup>1,4</sup>, LI Lingling<sup>1,5</sup>, WU Lunqiao<sup>1,6</sup>, LIN Haiying<sup>1</sup>, PAN Jianru<sup>1</sup>

1 College of Biological Science and Engineering, Fuzhou University, Fuzhou 350108, Fujian, China

2 Laboratory of Radiation Biology and Oncology, Fujian Medical University Cancer Hospital & Fujian Cancer Hospital, Fuzhou 350014, Fujian, China

3 College of Chemistry, Fuzhou University, Fuzhou 350108, Fujian, China

4 Yabo Jierui (Xiamen) Medical Technology Co. Ltd., Xiamen 361028, Fujian, China

5 Fuzhou Jiehe Biotechnology Co. Ltd., Fuzhou 350108, Fujian, China

6 Shenzhen Hemin Biotechnology Co. Ltd., Shenzhen 518116, Guangdong, China

**Abstract:** Antioxidant enzymes fused with cell-penetrating peptides could enter cells and protect cells from irradiation damage. However, the unselective transmembrane ability of cell-penetrating peptide may also bring antioxidant enzymes into tumor cells, thus protecting tumor cells and consequently reducing the efficacy of radiotherapy. There are active matrix metalloproteinase (MMP)-2 or MMP-9 in most tumor cellular microenvironments. Therefore, a fusion protein containing an MMP-2/9 cleavable substrate peptide X, a cell-penetrating peptide R9, a glutathione S-transferase (GST), and a human Cu, Zn superoxide dismutase (SOD1), was designed and named GST-SOD1-X-R9. In the tumor microenvironment, GST-SOD1-X-R9 would lose its cell-penetrating peptide and could not enter tumor cells due to the cleavage of substrate X by active MMP-2/9, thereby achieving selected entering normal cells. The complete nucleotide sequence of SOD1-X-R9 was synthesized and inserted into the prokaryotic expression vector pGEX-4T-1. The pGEX4T-1-SOD1-X-R9 recombinant plasmid was obtained, and soluble expression of the fusion protein was achieved. GST-SOD1-X-R9 was purified by ammonium sulfate precipitation and GST affinity chromatography. The molecular weight of the fusion protein was approximately 47 kDa, consistent with the theoretical value. The SOD and GST activities were 2 954 U/mg and 328 U/mg, respectively. Stability test suggested that almost no change in either SOD activity or GST activity of GST-SOD1-X-R9 was observed under physiological conditions. The fusion protein could be partially digested by collagenase IV in solution. Subsequently, the effect of MMP-2/9 activity on transmembrane ability of the fusion protein

was tested using 2D and 3D cultured HepG2 cells. Little extracellular MMP-2 activity of HepG2 cells was observed under 2D culture condition. While under the 3D culture model, the size and the MMP-2 activity of the HepG2 tumor spheroid increased daily. GST-SOD1-R9 proteins showed the same transmembrane efficiency in 2D cultured HepG2 cells, but the transmembrane efficiency of GST-SOD1-X-R9 in 3D cultured HepG2 spheres was reduced remarkably. This study provided a basis for further investigating the selectively protective effect of GST-SOD1-X-R9 against oxidative damage in normal cells.

**Keywords:** antioxidant enzyme; MMP-2/9 sensitive; cell permeable; expression in *Escherichia coli*; purification; stability

Redundant reactive oxygen species (ROS) encompass oxygen free radicals, and non-radical oxidants can cause lipid peroxidation, DNA damage, and protein denaturation, potentially inducing pathology. The primary and most abundant ROS is the superoxide anion radical, with a comparatively high oxidative capacity. The enzyme superoxide dismutase (SOD, EC 1.15.1.1) alternately catalyzes the dismutation of the superoxide ( $O_2^-$ ) radicals into molecular oxygen and hydrogen peroxide ( $H_2O_2$ ). Then, the  $H_2O_2$  is enzymatically converted by catalase and glutathione peroxidase into molecular oxygen and  $H_2O$ . In mammals, three SOD isoforms are found in living cells, including CuZn-SOD (SOD1) in the cytosol<sup>[1]</sup>, Mn-SOD (SOD2) in the mitochondrial matrix<sup>[2]</sup>, and EC-SOD (SOD3) in the extracellular space<sup>[3]</sup>. As the only natural enzymes that eliminate superoxide anions, SODs play a critical role in cellular defenses against oxidative damage<sup>[4]</sup>. However, it is less effective against intracellular ROS, as it is too large to enter cells freely.

The HIV-1 Tat protein transduction domain, TAT (YGRKKRRQRRR), was shown to carry large molecules, such as full-length proteins, across cellular membranes in both *in vitro* and *in vivo* models<sup>[5-10]</sup>. Previously, we constructed a cell membrane permeable SOD with the fusion of hCuZn-SOD (SOD1) and the cell-penetrating peptide TAT. The fusion protein SOD1-TAT was purified and crystallized, proving effective in preventing and treating the damage caused by single-dose UVB radiation on guinea pig

skins<sup>[11-13]</sup> and radiation-induced lung injury in mice<sup>[14]</sup>. As superoxide anion radicals are not the only ROS that can cause oxidative damage, we constructed a bifunctional antioxidant enzyme by fusing glutathione S-transferase (GST), SOD1, and TAT, namely, GST-TAT-SOD1. GST is an antioxidant enzyme that links toxic compounds with glutathione (GSH), thus forming less reactive compounds. In addition, the GST fusion could enhance the expression of soluble bifunctional antioxidant enzymes and simplify its purification. The bifunctional antioxidant enzyme has a better radioprotective effect than that of SOD1-TAT *in vitro*<sup>[15]</sup>. It was safe and provided good protection in mice exposed to whole-body ionizing irradiation<sup>[16]</sup>. Then, we enhanced the transduction efficiency of the bifunctional antioxidant enzyme by replacing the TAT peptide with a more efficient TAT derivative R9, a polyarginine with nine arginines, and named the resulting fusion protein GST-SOD1-R9<sup>[17]</sup>.

Although the bifunctional antioxidant enzyme can enter cells freely, its application in cancer therapy is limited because of the non-selective transmembrane effect of TAT or the R9 peptide<sup>[18]</sup>. Therefore, we further improved the bifunctional antioxidant enzyme according to the characteristics of the tumor microenvironment. Matrix metalloproteinases (MMPs) are proteases that hydrolyze components of the extracellular matrix. MMP-2, or MMP-9, or both, is expressed or overexpressed in almost all types of tumors and thus are a marker of malignancy<sup>[19]</sup>. Tsien's group proposed an MMP-2/9 cleavable linker

peptide X (PLGLAG) and constructed activatable cell-penetrating peptides (ACPPs) containing an anionic peptide domain (D9), the linker peptide X, and the cell permeating peptide R9 for tumor-specific delivery of cargo. The ACPPs have been successfully used as molecular imaging probes in tumor detection and intraoperative guidance<sup>[20-22]</sup>.

Since the linker peptide X is recognized and hydrolyzed by MMP-2/9, we weakened the tumor cell-permeable ability of GST-SOD1-R9 by modifying the protein with an insert of the linker peptide X before R9 and named this construct GST-SOD1-X-R9. Here we report the construction and expression of the novel multifunctional antioxidant enzyme, GST-SOD1-X-R9. Additionally, we report the purification, stability, cell permeability and enzymatic-triggered cleavage of GST-SOD1-X-R9 to gain basic knowledge for the use of the fusion protein in future studies and applications.

## 1 Materials and methods

### 1.1 Materials

*Escherichia coli* (*E. coli*) DH5 $\alpha$  competent cells and B27 were purchased from Invitrogen (Carlsbad, CA). The *E. coli* expression strain, BL21 (DE3), was purchased from Novagen (now EMD Millipore, Billerica, MA). The pGEX-4T-1 plasmid was purchased from GE Healthcare (USA). All restriction enzymes were purchased from Promega (USA). A GST affinity chromatography resin was purchased from Sangon Biotech (Shanghai, China). The SOD and GST reagent kits were purchased from Nanjing Jiancheng Bioengineering (Jiangsu, China). Micro BCA<sup>TM</sup> Protein Assay Kit was purchased from Thermo Scientific (USA). FITC, collagenase IV, aminophenylmercuric acetate (APMA), and gelatin were purchased from Sigma (USA). DMEM and fetal bovine serum (FBS) were purchased from HyClone (USA) and PAN (Germany), respectively. Antibiotic-antimycotic and DME/F12 were purchased from Life

Technologies (USA). All other chemicals were of analytical purity. The Human hepatocellular carcinoma HepG2 was received from the Shanghai Institute of Biochemistry and Cell Biology, Chinese Academy of Sciences (SIBCB, CAS, China). bFGF and EGF were purchased from PeproTech (USA). Matrigel matrix was purchased from BD Biosciences (San Jose, CA, USA).

### 1.2 Methods

#### 1.2.1 Synthesis of the SOD1-X-R9 gene

The nucleotide sequence of human SOD1 (GenBank: X02317.1), fused with the MMPs cleavable linker peptide X (PLGLAG) and the R9 cell-penetrating peptides (RRRRRRRRR), was synthesized by Sangon Biotech (Shanghai, China) according to the preferred codon usage of *E. coli* to increase the final protein expression yield.

#### 1.2.2 Construction of the prokaryotic expression vector pGEX-4T-1-SOD1-X-R9

Double restriction endonuclease digestion using *EcoR* I and *Xho* I was performed on the pGEX-4T-1 expression vector and the target gene followed by digested product purification using a QIAquick Gel Extraction kit (Qiagen, Germany). The plasmid and digested target fragment were ligated at 16 °C for 4 h with T4 DNA ligase (Promega, USA) and transformed into an *E. coli* (DH5 $\alpha$ ) bacterial strain by heat shock at 42 °C for 60 s. The colonies grown on agar plates were selected and seeded separately in fresh culture tubes. Then, single clones from each transformation were incubated with shaking (220 r/min) at 37 °C overnight. Subsequently, plasmid purification was performed using a QIAprep Spin Miniprep kit (Qiagen, Germany). The resulting plasmid, pGEX-4T-1-SOD1-X-R9, was verified by both *EcoR* I and *Xho* I double restriction endonuclease digestions and subsequent sequencing (Sangon, China).

#### 1.2.3 Expression of GST-SOD1-X-R9

The recombinant plasmid was transformed into *E. coli* strain BL21(DE3) to express GST-SOD1-X-R9. Cells were cultured in LB medium supplemented with 50 mg/mL ampicillin

at 37 °C at 200 r/min. When the  $OD_{600}$  of the culture reached a value of 0.6–0.8,  $CuSO_4$  and  $ZnSO_4$  were added at a final concentration of 0.5 mmol/L and 0.1 mmol/L, respectively. Then, isopropyl  $\beta$ -D-1-thiogalactopyranoside (IPTG) was added to a final concentration of 0.2 mmol/L to induce protein expression. Different induction conditions, including induction times from 0–12 h and temperatures from 16–37 °C, were conducted to optimize the heterologous protein expression in *E. coli*.

After induction, the recombinant protein expression was terminated by centrifuging the solution at 10 000 r/min at 4 °C for 5 min to collect the cells. Then, the harvested cells were resuspended in phosphate-buffered saline (PBS) and lysed by ultrasonication (VC-750, Sonic Solutions Co., USA), and the lysate was centrifuged at 12 000 r/min, at 4 °C for 20 min. The supernatant of the lysate and unlysed cells were analyzed by 12.5% SDS-polyacrylamide gel electrophoresis (PAGE).

#### 1.2.4 Purification using affinity chromatography

Bacteria were washed in PBS and lysed in buffer A (10 mmol/L  $Na_2HPO_4$ , 1.8 mmol/L  $KH_2PO_4$ , 2.7 mmol/L KCl, pH 7.3) using a cell disrupter (VC-750, Sonic Solutions Co., USA). The supernatant (crude extract) was collected after centrifugation of the lysate for 20 min at 12 000 r/min in a HITACHI RX series himac CF15RX rotor at 4 °C. The supernatant containing GST-SOD1-X-R9 was precipitated by incubation with 56.1 g ammonium sulfate per 100 mL at 4 °C. For purification of GST-SOD1-X-R9, the precipitate was resuspended in 20 mmol/L PBS, pH 7.4, and purified by a GST affinity chromatography resin according to the manufacturer's instructions. After binding and washing, the bound protein was eluted with 50 mmol/L Tris-HCl containing 0.01 mol/L glutathione, pH 8.0. The concentration of the purified protein was determined by a BCA<sup>TM</sup> protein assay kit using BSA as a standard protein. The SOD activity and GST activity of the purified protein were assayed with SOD and GST reagent

kits, respectively. The purity of proteins was analyzed by Image J software (NIH, Bethesda, MD, USA) using a stained SDS-PAGE.

#### 1.2.5 pH stability

The protein solution was aliquoted and adjusted to different pH values using a series of buffers (buffer contained 6.008 g citric acid, 3.893 g  $KH_2PO_4$ , 1.769 g boric acid, and 5.266 g barbitone per liter and was titrated with 0.2 mol/L NaOH from pH 4 to pH 9) at 4 °C for 30 min. Then, the samples were brought back to room temperature (25 °C) before use. Their residual SOD activity and GST activity were subsequently determined by the SOD and GST reagent kits, respectively.

#### 1.2.6 Thermal stability

The protein solution was aliquoted and incubated at different temperatures (25–80 °C) in 20 mmol/L PB (0.02 mol/L phosphate buffer pH 7.0) for 30 min. Then, they were cooled to room temperature (25 °C) before use. The residual SOD activity and GST activity were determined by the SOD and GST reagent kits, respectively.

#### 1.2.7 Enzymatic-triggered cleavage of GST-SOD1-X-R9 by MMPs

To analyze the enzymatic cleavage of the MMP-2/9 sensitive linker peptide X, GST-SOD1-X-R9 cleavage was studied in the presence of collagenase IV (1.0 mg/mL). Firstly, 50  $\mu$ L collagenase IV was activated with 10  $\mu$ L APMA solution (10 mmol/L) for 1 h at 37 °C. Then, 50  $\mu$ L GST-SOD1-X-R9 (1.2 mg/mL) was mixed with an equivalent volume of PBS or activated collagenase IV and incubated at 37 °C for 3 h. The aliquots were subsequently analyzed using 12.5% SDS-PAGE.

#### 1.2.8 MMP-2 activity of HepG2 cells in 2D or 3D culture

HepG2 cells were pre-cultured in DMEM supplemented with 10% FBS and 1% antibiotic-antimycotic at 37 °C in a  $CO_2$  incubator for 24 h. After pre-culture, 100  $\mu$ L of HepG2 cell suspension ( $1.0 \times 10^4$  cells/mL) was applied to a 24-well flat-bottom plate (Corning, USA) for 2D culture for 24 h. Three-dimensional spheroid cells

were cultured in ultra-low attachment 24-well flat-bottom plates (Corning, USA) in DMEM/F12 supplemented with 20 ng/mL epidermal growth factor, 20 ng/mL basic fibroblast growth factor, 2% B27, 2% Matrigel, and 1% antibiotic-antimycotic. The cell concentration was the same as that in the 2D culture and the cells were cultured at 37 °C in a CO<sub>2</sub> incubator for 1–7 days. The formation of HepG2 spheroid in 3D cultures was monitored using the inverted microscope (Axio Observer A1, Carl Zeiss, Germany).

The activity of MMP-9 and MMP-2 was assessed by gelatin zymography. The 2D or 3D culture supernatants of HepG2 cells without serum from each sample were mixed with loading buffer and subjected to SDS-PAGE containing 0.1% gelatin. Then gels were stained with Coomassie brilliant blue R-250.

### 1.2.9 Translocation of GST-SOD1-X-R9 *in vitro*

The fusion proteins were labeled using fluorescein isothiocyanate (FITC), according to the method of our previous work<sup>[15]</sup>. The 2D or 3D cultured HepG2 cells were washed by PBS 3 times and incubated with 400 μL 0.25 mg/mL fusion proteins for 3 h, subsequently. Then, the cells were washed by PBS for 5 times and lysed by cell lysis buffer (0.5% Triton X-100 and 0.1% SDS). Finally, accumulation of the fluorescence intensity in HepG2 cells was detected by a Synergy H4 Hybrid Multi-Mode Microplate Reader (BioTek Instruments, Winooski, VT, USA) and used to confirm the cell-penetrating ability of the fusion protein as described in ref. [15]. Following the manufacturer's directions, the protein was determined by a BCA<sup>TM</sup> protein assay kit. The fluorescence intensity was corrected for background signal, normalized for protein content, and expressed as the fluorescence/mg of protein to normalized fluorescence per cell.

### 1.2.10 Statistical analyses

Statistical analysis of all data was performed using Excel or prism. The results are reported as means±SD. The *P* values were determined using the Student Two-tailed *t*-test, and *P*<0.05 was considered statistically significant.

## 2 Results and discussion

### 2.1 Construction of the expression vector

The polypeptide sequence was optimized according to *E. coli* codon usage and the oligonucleotide was synthesized by Sangon Biotech (China). Then, the synthesized target DNA fragment was ligated into the pGEX-4T-1 vector to construct the expression vector pGEX-4T-1-SOD1-X-R9 (Figure 1). The newly generated plasmid was then digested with the restriction endonucleases, *EcoR* I and *Xho* I. Gel electrophoresis (Figure 2) showed the cleavage by *EcoR* I and *Xho* I generated a target fragment consistent with the size of the expected gene fragment (510 bp). The endonuclease cleavage fragment was verified by sequencing, and the sequencing results were consistent with the SOD1-X-R9 sequence, indicating the successful construction of the expression vector.

### 2.2 Expression of the GST-SOD1-X-R9 recombinant protein

After transforming the pGEX-4T-1-SOD1-X-R9 construct into *E. coli* BL21(DE3), protein expression was induced by IPTG. To improve the

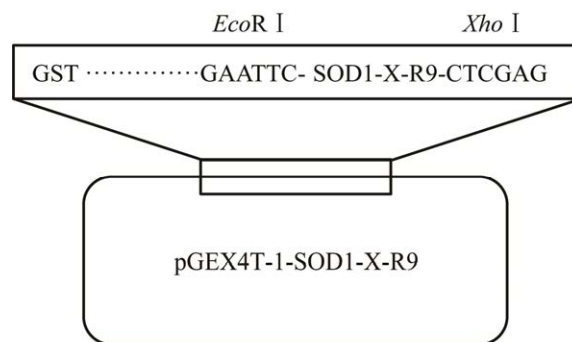


图 1 pGEX-4T-1-SOD1-X-R9 重组表达载体示意图

Figure 1 Schematic map of the recombinant expression vector pGEX-4T-1-SOD1-X-R9. The SOD1-X-R9 gene was cloned into pGEX-4T-1 using *EcoR* I and *Xho* I sites as described in the materials and methods.

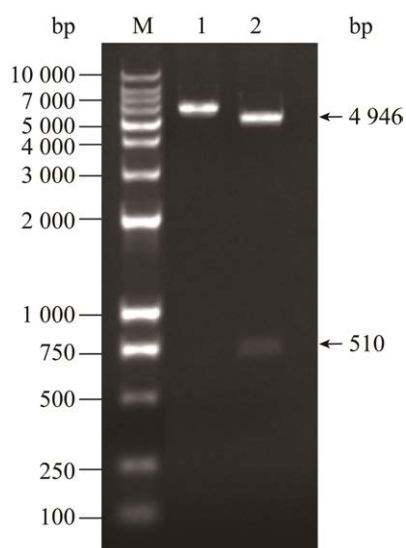


图2 *EcoR* I 和 *Xho* I 双酶消化后重组质粒的凝胶电泳

Figure 2 Gel electrophoresis of the recombinant plasmid following *EcoR* I and *Xho* I double enzymatic digestion. M: marker; 1: pGEX4T-1-SOD1-X-R9; 2: double digested fragment.

expression of the soluble recombinant GST-SOD1-X-R9, we investigated the effects of various parameters, such as induction time and growth temperatures.

Optimal incubation time can vary depending on the target protein and the choice of the expression system. To establish an optimum

induction time for GST-SOD1-X-R9 expression, aliquots of induced cultures were taken at regular intervals post-induction and analyzed by SDS-PAGE. As shown in Figure 3, the expression of GST-SOD1-X-R9 increased with induction time, and the soluble expression of GST-SOD1-X-R9 reached the highest at 6 h.

To identify an ideal expression temperature for GST-SOD1-X-R9, an initial culture of GST-SOD1-X-R9 expressing cells was divided into five aliquots immediately after induction and grown for a further 6 h at 16 °C, 20 °C, 25 °C, 30 °C, and 37 °C. SDS-PAGE analysis (Figure 4) showed that all these temperatures suited GST-SOD1-X-R9 expression. Nevertheless, 25 °C was the best temperature for soluble GST-SOD1-X-R9 production, as the expression of GST-SOD1-X-R9 was the highest at this temperature. Induction with 0.2 mmol/L IPTG at 25 °C for 6 h resulted in the most abundant expression of soluble protein.

### 2.3 Purification and identification of the GST-SOD1-X-R9 recombinant protein

After identifying the optimal conditions for expression of the fusion protein, these conditions were employed for growing larger cultures of the recombinant strain. As is shown in Figure 5 and Table 1, the fusion protein was purified by ammonium sulfate precipitation and subsequent

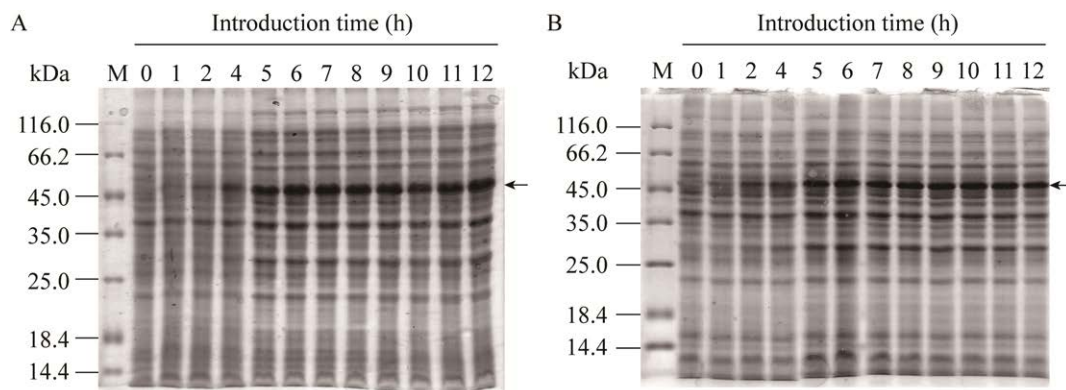


图3 不同诱导时间下 GST-SOD1-X-R9 表达的 SDS-PAGE 分析

Figure 3 SDS-PAGE of GST-SOD1-X-R9 expression with different induction time. (A) Total protein. (B) Soluble fractions. M: protein weight marker; ←: GST-SOD1-X-R9.

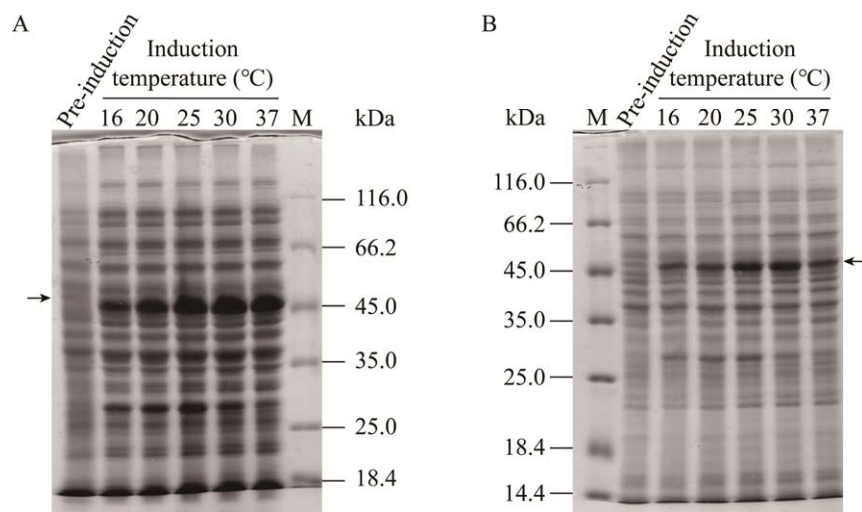


图4 不同诱导温度下 GST-SOD1-X-R9 表达的 SDS-PAGE 分析

Figure 4 SDS-PAGE of GST-SOD1-X-R9 expression under different induction temperature. (A) Total protein. (B) Soluble fractions. M: protein weight marker; ←: GST-SOD1-X-R9.

GST affinity chromatography. SDS-PAGE revealed that the size of the purified protein was 47 kDa, which almost matched its predicted size of 46 kDa (Figure 5), with about 95% purity. After ultrafiltration and dialysis, the final SOD activity and GST activity of the purified protein were 2 954 U/mg and 328 U/mg, respectively. According to the correct

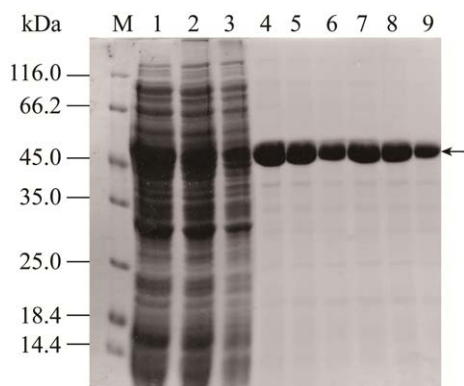


图5 GST-SOD1-X-R9 融合蛋白的纯化

Figure 5 Purification of the GST-SOD1-X-R9 fusion protein. 1: crude extract; 2: precipitation of crude extract with 80% ammonium sulfate; 3: flow-through of GST affinity chromatography resin; 4-9: elutions of GST affinity chromatography resin; M: protein marker; ←: GST-SOD1-X-R9.

molecular weight and the special antioxidant activity, the purified fusion protein was confirmed to be GST-SOD1-X-R9. The SOD and GST activities of GST-SOD1-X-R9 were higher than those of GST-SOD1-R9 with a SOD activity of 2 388 U/mg and GST activity of 227 U/mg<sup>[17]</sup>. The higher antioxidant activities of GST-SOD1-X-R9 may be due to the additionally inserted X linker peptide, which reduced the adverse effect of the R9 peptide in the structure of GST-SOD1.

#### 2.4 pH stability

The pH stability of the antioxidant activities of GST-SOD1-X-R9 was determined by performing an assay in a series of buffers with intervals of 1 pH unit at 4 °C for 30 min, as shown in Figure 6. Results revealed that the antioxidant activities of GST-SOD1-X-R9 were stable between pH 5.0 and 9.0 and best stable at pH 7.0. At that pH, 100% of the antioxidant activities was retained. While at low pH (pH<5.0), the antioxidant activities were reduced rapidly.

Compared with GST-SOD1-R9<sup>[17]</sup>, the antioxidant activities of GST-SOD1-X-R9 were stable at a more comprehensive pH range. Moreover, the residual enzyme activity of the latter was higher than that of the former under

表 1 GST-SOD1-X-R9 蛋白纯化结果

Table 1 Summary of the purification process of GST-SOD1-X-R9 protein

Steps	Total protein (mg)	Total SOD activity (units)	Specific SOD activity (units/mg)	SOD yield (%)	Total GST activity (units)	Specific GST activity (units/mg)	GST yield (%)	Purity (%)
Crude extract	336	198 303	589	100	24 950	74	100	31
80% Ammonium sulfate	201	147 233	733	74	19 337	97	77	35
GST column (elutions)	72	83 623	1 162	42	11 955	166	48	95

From 5.37 g (wet weight) of cell pellet collected from 900 mL of bacterial culture.

alkaline conditions. The enhancement of the pH stability of GST-SOD1-X-R9 may be due to the addition of the X linker peptide.

## 2.5 Thermal stability

The thermal stability of GST-SOD1-X-R9 were analyzed after pre-incubation of GST-SOD1-X-R9 at different temperatures (25–80 °C) for 30 min. As shown in Figure 7, the GST activity of the fusion protein was stable between 25 °C and 50 °C. The activity reduced at incubation temperatures higher than 50 °C, and was almost zero after 30 min incubation at 80 °C. These results indicated that

the GST activity of the fusion protein exhibited moderate thermal stability. The SOD activity decreased slowly with increased temperature until 60 °C, and dropped rapidly at temperatures higher than 60 °C, and only less than 10% of the activity remained at 80 °C.

Compared with GST-SOD1-R9<sup>[17]</sup>, the residual SOD activity of GST-SOD1-X-R9 was slightly lower at incubation temperatures between 25 °C and 50 °C. Higher residual SOD activity of the latter was observed at temperatures exceeding 50 °C. Unlike SOD activity, the residual GST activity of GST-SOD1-X-R9 was slightly higher

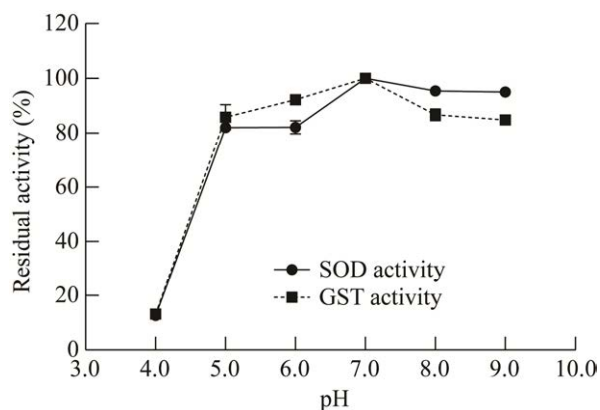


图 6 pH 对 GST-SOD1-X-R9 抗氧化酶稳定性的影响

Figure 6 Effect of pH on the stability of GST-SOD1-X-R9. The purified protein was aliquoted in buffers adjusted to different pH values and incubated at 4 °C for 30 min. After incubation, the samples were brought back to room temperature (25 °C), and relative reagent kits determined the remaining activities. Data are  $\bar{x} \pm s$  from three replications.

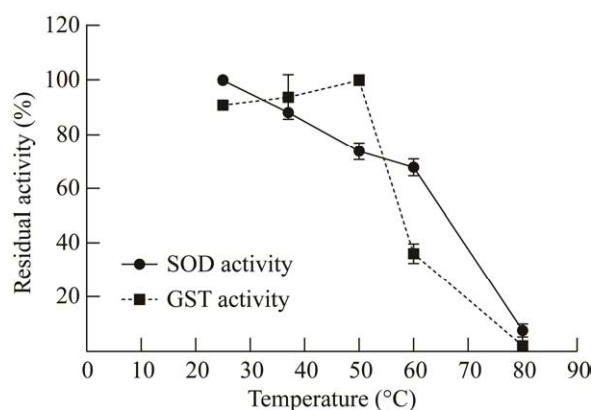


图 7 温度对 GST-SOD1-X-R9 抗氧化酶稳定性的影响

Figure 7 Effect of temperature on the stability of GST-SOD1-X-R9. The purified protein was aliquoted and incubated at 25–80 °C for 30 min. After incubation, the samples were cooled to room temperature (25 °C), and the remaining activities was determined by relevant reagent kits. Data are  $\bar{x} \pm s$  from three replications.

than that of GST-SOD1-R9<sup>[17]</sup> at incubation temperatures between 25 °C and 50 °C. The two fusion proteins shared the same trends at higher thermal treatment temperatures. These results hint at the complicated effect of the X linker peptide on the fusion protein structure.

## 2.6 Enzymatic-triggered cleavage of GST-SOD1-X-R9

GST-SOD1-X-R9 contains an MMP-2/9-sensitive linker peptide X. Subsequently, the triggered cleavage study was performed through an enzymatic digestion experiment for 3 h, and the results are shown in Figure 8. GST-SOD1-X-R9 had no change when simply mixed with PBS (lane 3) or incubated in PBS at 37 °C for 3 h (lane 4) without activated collagenase IV. In contrast, the reduction in the molecular weight of GST-SOD1-X-R9 was observed in lane 5 when the fusion protein was incubated with activated collagenase IV at 37 °C for 3 h. The result of lane 5 reflected partial degradation of the fusion protein which partly proved that MMP-2/9 could cleave GST-SOD1-X-R9.

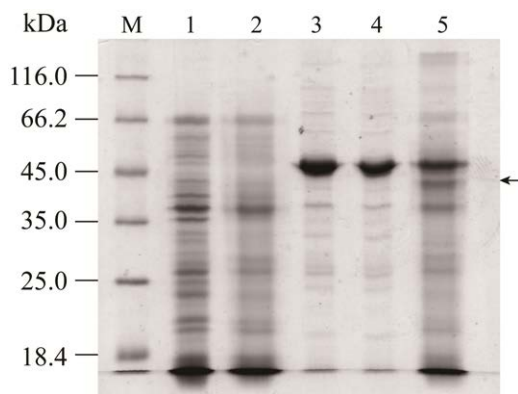


图 8 GST-SOD1-X-R9 的酶促水解

Figure 8 Enzymatic-triggered cleavage of GST-SOD1-X-R9. M: protein marker; 1: Inactivated collagenase IV; 2: Activated collagenase IV; 3: GST-SOD1-X-R9 mixed with PBS; 4: GST-SOD1-X-R9 incubated in PBS at 37 °C for 3 h; 5: GST-SOD1-X-R9 incubated with activated collagenase IV at 37 °C for 3 h; ←: enzymatic hydrolysate of GST-SOD1-X-R9.

The components of collagenase IV were not only MMP-2/9, which may influence it to act as purified MMP-2/9. The *in vitro* enzymatic-triggered cleavage may not reflect the real state of the fusion protein in the tumor microenvironment. Therefore, a hepatoma carcinoma cell-expressed low level of MMP-2, HepG2, was selected to further examine whether the transduction of GST-SOD1-X-R9 is sensitive to the MMP-2 activity of the tumor microenvironment.

## 2.7 MMP-2 activity of HepG2 cells in 2D or 3D cultures

As shown in Figure 9, there was no MMP-9 activity but little MMP-2 activity in 2D culture medium of HepG2 (Figure 9A). However, when the HepG2 cells were cultured in a 3D culture condition, they were susceptible in the medium as single-cell suspension on the 1st day and began to assemble into tumor spheroid on the 3rd day. The size of HepG2 tumorspheres was increased gradually with the culture time (Figure 9C). Consequently, the MMP-2 activity of HepG2 spheroid was progressively increased with the culture time (Figure 9B).

## 2.8 Translocation of recombination protein GST-SOD1-X-R9 *in vitro*

To estimate the MMP-2/9 sensitive transduction of GST-SOD1-X-R9, three fusion proteins were labeled with FITC, respectively, internalized into cultured cells, and quantified by a fluorescence microplate reader. As shown in Figure 10, compared with untreated cells, the fluorescence intensity of GST-SOD1 treated cells did not considerably increase after incubation for 3 h, both in 2D or 3D cultures. GST-SOD1-R9 and GST-SOD1-X-R9 can enter 2D cultured HepG2 cells efficiently without significant difference. Two fusion proteins showed a marked differentiation in 3D cultured HepG2 spheroid cells. GST-SOD1-R9 translocated into the HepG2 spheroid cells as efficiently as the 2D cultured cells ( $P < 0.0001$ ) did. However, the 3D cell-permeability of GST-SOD1-X-R9 remarkably decreased compared with that of GST-SOD1-R9 ( $P < 0.0001$ ).

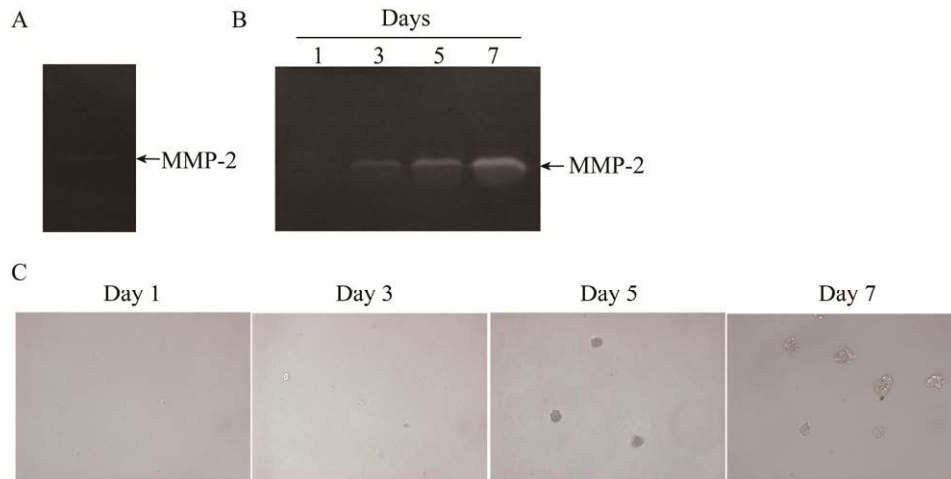


图9 HepG2 细胞在 2D (A) 或 3D (B) 培养条件下的 MMP-2 活性以及肿瘤球体形成 (C)

Figure 9 The MMP-2 activity of HepG2 cells in 2D (A) or 3D (B) cultures and the formation of tumor spheroid (C).

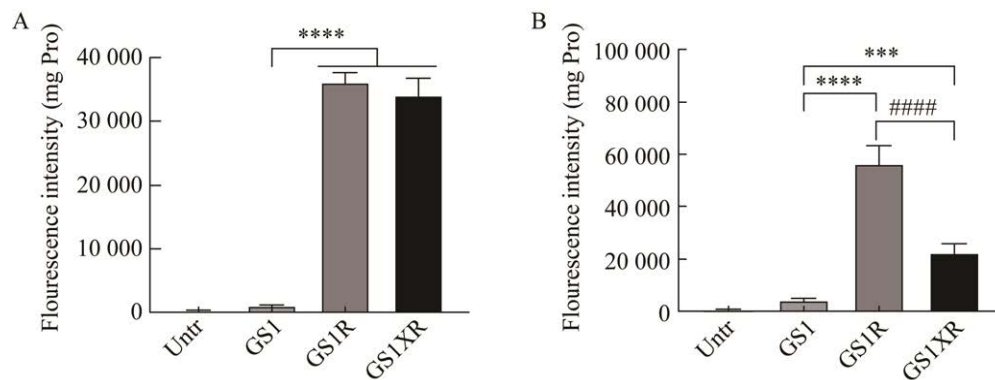


图10 GST-SOD1-X-R9 融合蛋白在 2D (A) 或 3D (B) 培养的 HepG2 细胞中的跨膜情况

Figure 10 Translocation of the GST-SOD1-X-R9 fusion protein in 2D (A) or 3D (B) cultured HepG2 cells. The bars indicate the  $\bar{x} \pm s$ . ( $n=3$ , compared with Untr group, \*\*\*:  $P<0.001$ , \*\*\*\*:  $P<0.0001$ ; compared with GS1 group, #####:  $P<0.0001$ ).

This indicated the increased MMP-2 activity of 3D cultured tumor spheroid cells effectively weakened the 3D cell-permeability of GST-SOD1-X-R9.

GST-SOD-X-R9 can enter normal cells freely due to the transduction activities of the R9 peptide. However, GST-SOD-X-R9 would lose the cell-permeating ability in the tumor microenvironment as the R9 peptide was lost with the cleavage of linker peptide X by MMP-2/9 excreted from tumor cells. As a marker of

malignancy, MMP-2/9 is essential for tumor growth and overexpressed in almost all types of tumors, including skin melanoma<sup>[23]</sup>, lung carcinoma<sup>[24]</sup>, ovarian carcinoma<sup>[25]</sup>, brain neoplasms<sup>[26]</sup>, and breast carcinoma<sup>[27]</sup>. Some tumor cells seem to have less expression of MMP-2/9, such as HepG2. In contrast, they increased their MMP-2/9 expression during forming tumor spheroid. Hence, as expected, GST-SOD-X-R9 will be hard to permeate the solid tumors. The selective cell-permeating

ability and bifunctional antioxidant activity of GST-SOD1-X-R9 make it a potentially promising protector as an adjuvant to radiotherapy or chemotherapy for tumor treatment.

### 3 Conclusion

In summary, we have expressed the soluble GST-SOD1-X-R9 fusion protein. Optimized expression conditions can enhance the expression quantity of the fusion protein. The fusion protein was purified by GST affinity chromatography and identified based on SDS-PAGE and antioxidant activity analysis. The purified fusion protein was stable under physiological conditions. Finally, the GST-SOD1-X-R9 fusion protein can be cleaved by MMPs, it had good cell-permeability in 2D cultured cells, but poor cell-permeability in 3D cultured tumor cells expressed MMP-2. The present work lays the foundation for the future application of GST-SOD1-X-R9 to be an adjuvant of radiotherapy or chemotherapy for tumor treatment.

### REFERENCES

- [1] Fridovich I. Superoxide dismutases. *Adv Enzymol Relat Areas Mol Biol*, 1974, 41(0): 35-97.
- [2] Weisiger RA, Fridovich I. Mitochondrial superoxide dismutase: site of synthesis and intramitochondrial localization. *J Biol Chem*, 1973, 248(13): 4793-4796.
- [3] Marklund SL. Extracellular superoxide dismutase and other superoxide dismutase isoenzymes in tissues from nine mammalian species. *Biochem J*, 1984, 222(3): 649-655.
- [4] Riley PA. Free radicals in biology: oxidative stress and the effects of ionizing radiation. *Int J Radiat Biol*, 1994, 65(1): 27-33.
- [5] Eguchi A, Akuta T, Okuyama H, et al. Protein transduction domain of HIV-1 Tat protein promotes efficient delivery of DNA into mammalian cells. *J Biol Chem*, 2001, 276(28): 26204-26210.
- [6] Josephson L, Tung CH, Moore A, et al. High-efficiency intracellular magnetic labeling with novel superparamagnetic-Tat peptide conjugates. *Bioconjug Chem*, 1999, 10(2): 186-191.
- [7] Lewin M, Carlesso N, Tung CH, et al. Tat peptide-derivatized magnetic nanoparticles allow *in vivo* tracking and recovery of progenitor cells. *Nat Biotechnol*, 2000, 18(4): 410-414.
- [8] Rothbard JB, Garlington S, Lin Q, et al. Conjugation of arginine oligomers to cyclosporin A facilitates topical delivery and inhibition of inflammation. *Nat Med*, 2000, 6(11): 1253-1257.
- [9] Torchilin VP, Rammohan R, Weissig V, et al. TAT peptide on the surface of liposomes affords their efficient intracellular delivery even at low temperature and in the presence of metabolic inhibitors. *Proc Natl Acad Sci USA*, 2001, 98(15): 8786-8791.
- [10] Wadia JS, Dowdy SF. Protein transduction technology. *Curr Opin Biotechnol*, 2002, 13(1): 52-56.
- [11] Pan JR, Peng SM, Zhou JH, et al. Protective effects of recombinant protein PTD-SOD on Guinea pigs damaged by ultraviolet B. *Radiat Protect*, 2010, 30(5): 284-288 (in Chinese).
- [12] Pan JR, Zhou JH, Peng SM, et al. The preventing effects of recombinant protein PTD-SOD on Guinea pigs damaged by ultraviolet B. *J Radiat Res Radiat Process*, 2009, 27(5): 297-302 (in Chinese).
- [13] Pan JR, Zhou KJ, Zheng GJ, et al. Crystallization and preliminary X-ray diffraction analysis of the SOD-TAT fusion protein. *Acta Cryst Sect F*, 2012, 68(5): 543-546.
- [14] Pan JR, Su Y, Hou XJ, et al. Protective effect of recombinant protein SOD-TAT on radiation-induced lung injury in mice. *Life Sci*, 2012, 91(3/4): 89-93.
- [15] Pan JR, He HC, Su Y, et al. GST-TAT-SOD: cell permeable bifunctional antioxidant enzyme—a potential selective radioprotector. *Oxid Med Cell Longev*, 2016, 2016: 5935080.
- [16] Pan JR, He HC, Su Y, et al. *In vivo* radioprotective activity of cell-permeable bifunctional antioxidant enzyme GST-TAT-SOD against whole-body ionizing irradiation in mice. *Oxid Med Cell Longev*, 2017, 2017: 2689051.
- [17] 潘剑茹, 吴伦巧, 何火聪, 等. GST-SOD1-R9 融合蛋白的表达、纯化、稳定性与跨膜效应. *生物工程学报*, 2017, 33(5): 828-837.  
Pan JR, Wu LQ, He HC, et al. Expression, purification, stability and transduction efficiency of GST-SOD1-R9 fusion protein. *Chin J Biotech*, 2017, 33(5): 828-837 (in Chinese).
- [18] Dissanayake S, Denny WA, Gamage S, et al. Recent developments in anticancer drug delivery using cell penetrating and tumor targeting peptides. *J Control*

- Release, 2017, 250: 62-76.
- [19] Giaeleli C, Theocharis AD, Karamanos NK. Roles of matrix metalloproteinases in cancer progression and their pharmacological targeting. *FEBS J*, 2011, 278(1): 16-27.
- [20] Jiang T, Olson ES, Nguyen QT, et al. Tumor imaging by means of proteolytic activation of cell-penetrating peptides. *PNAS*, 2004, 101(51): 17867-17872.
- [21] Turner JJ, Arzumanov AA, Gait MJ. Synthesis, cellular uptake and HIV-1 Tat-dependent trans-activation inhibition activity of oligonucleotide analogues disulphide-conjugated to cell-penetrating peptides. *Nucleic Acids Res*, 2005, 33(1): 27-42.
- [22] Butterfield SM, Miyatake T, Matile S. Amplifier-mediated activation of cell-penetrating peptides with steroids: multifunctional anion transporters for fluorogenic cholesterol sensing in eggs and blood. *Angew Chem Int Ed Engl*, 2009, 48(2): 325-328.
- [23] Väisänen A, Kallioinen M, Taskinen PJ, et al. Prognostic value of MMP-2 immunoreactive protein (72 kD type IV collagenase) in primary skin melanoma. *J Pathol*, 1998, 186(1): 51-58.
- [24] Kodate M, Kasai T, Hashirnoto H, et al. Expression of matrix metalloproteinase (gelatinase) in T1 adenocarcinoma of the lung. *Pathol Int*, 1997, 47(7): 461-469.
- [25] Davidson B, Goldberg I, Gotlieb WH, et al. High levels of MMP-2, MMP-9, MT1-MMP and TIMP-2 mRNA correlate with poor survival in ovarian carcinoma. *Clin Exp Metastasis*, 1999, 17(10): 799-808.
- [26] Jääliinjä J, Herva R, Korpela M, et al. Matrix metalloproteinase 2 (MMP-2) immunoreactive protein is associated with poor grade and survival in brain neoplasms. *J Neurooncol*, 2000, 46(1): 81-90.
- [27] Puzovic V, Brcic I, Ranogajec I, et al. Prognostic values of ETS-1, MMP-2 and MMP-9 expression and co-expression in breast cancer patients. *Neoplasma*, 2014, 61(4): 439-446.

(本文责编 陈宏宇)